Neuron
Article

Drosophila Sensory Neurons Require Dscam for Dendritic Self-Avoidance and Proper Dendritic Field Organization

Peter Soba,[1,3] Sijun Zhu,[1,3] Kazuo Emoto,[1,4] Susan Younger,[1] Shun-Jen Yang,[2] Hung-Hsiang Yu,[2] Tzumin Lee,[2] Lily Yeh Jan,[1] and Yuh-Nung Jan[1,*]
[1] Howard Hughes Medical Institute, Departments of Physiology, Biochemistry, and Biophysics, University of California, San Francisco, Rock Hall, 1550 4th Street, San Francisco, CA 94143, USA
[2] Department of Neurobiology, University of Massachusetts Medical School, Worcester, MA 01605, USA
[3] These authors contributed equally to this work.
[4] Present address: Neural Morphology Laboratory, National Institute of Genetics, Yata 1111, Mishima 411-8540, Japan.
*Correspondence: yuhnung.jan@ucsf.edu
DOI 10.1016/j.neuron.2007.03.029

SUMMARY

A neuron's dendrites typically do not cross one another. This intrinsic self-avoidance mechanism ensures unambiguous processing of sensory or synaptic inputs. Moreover, some neurons respect the territory of others of the same type, a phenomenon known as tiling. Different types of neurons, however, often have overlapping dendritic fields. We found that *Down's syndrome Cell Adhesion Molecule* (*Dscam*) is required for dendritic self-avoidance of all four classes of *Drosophila* dendritic arborization (da) neurons. However, neighboring mutant class IV da neurons still exhibited tiling, suggesting that self-avoidance and tiling differ in their recognition and repulsion mechanisms. Introducing 1 of the 38,016 Dscam isoforms to da neurons in *Dscam* mutants was sufficient to significantly restore self-avoidance. Remarkably, expression of a common Dscam isoform in da neurons of different classes prevented their dendrites from sharing the same territory, suggesting that coexistence of dendritic fields of different neuronal classes requires divergent expression of Dscam isoforms.

INTRODUCTION

Proper sampling of sensory or synaptic inputs critically depends on the morphogenesis and organization of dendrites. Several mechanisms contribute to the orderly organization of dendritic fields of various types of neurons in a common area.

First, the dendrites of an individual neuron typically do not fasciculate or cross one another (self-avoidance). Given the likely local processing and integration of inputs impinging onto a dendritic branch (Jan and Jan, 2003; Stuart et al., 1999), the absence of overlap of a neuron's dendritic branches facilitates orderly projection of sensory or synaptic inputs for efficient and unambiguous signal processing. In addition, self-avoidance could also contribute to the maximal dispersion of dendritic branches for more uniform coverage of the entire dendritic field of a neuron.

Second, certain types of neurons exhibit a phenomenon known as tiling, which refers to the avoidance between dendrites of adjacent neurons of the same type. Tiling was first reported for the mammalian retinal ganglion cells (Perry and Linden, 1982; Wassle et al., 1981) and allows neurons of the same class to cover the entire dendritic field like tiles covering a floor: completely, but without redundancy.

Third, neurons of different types often have overlapping dendritic fields to allow different neuronal types to process different aspects of inputs. For example, different classes of retinal ganglion cells that selectively respond to motion in different directions need to cover the same visual field (Amthor and Oyster, 1995).

Drosophila dendritic arborization (da) neurons exhibit the full range of possible dendritic interactions, encompassing self-avoidance, tiling, and coexistence. Larval da neurons are sensory neurons of the peripheral nervous system and fall into four different classes with different morphology (Grueber et al., 2002). All classes display self-avoidance, while only two of the four classes of da neurons exhibit tiling; namely, the class III da neurons with characteristic dendritic spikes, and the class IV da neurons with the greatest dendritic complexity (Grueber et al., 2002, 2003; Sugimura et al., 2003). The simpler class I and class II da neurons have smaller dendritic fields that normally do not overlap with those of the same class. However, when class I neurons are duplicated in *hamlet* mutants, they occupy the same area and do not repel each other. In contrast, duplicated class IV neurons tile and hence subdivide the dendritic field (Grueber et al., 2003). Moreover, da neurons belonging to different

classes extensively share their dendritic fields (Gao et al., 2000; Grueber et al., 2002), analogous to the repeated coverage of the retina by different classes of retinal ganglion cells tuned to different features of the visual field (Rockhill et al., 2000). *Drosophila* da neurons thus present an opportunity to examine the role of molecular interactions between dendrites and serve as a useful model to study the mechanism of dendritic field organization.

The tiling phenomenon and self-avoidance both involve recognition and repulsion of dendrites. In recent years, the NDR family kinase Tricornered/Sax-1 (*trc*), its activator Furry/Sax-2 (*fry*), and the upstream Ste-20 family kinase Hippo (*hpo*) have been identified as important components of the intracellular signaling cascade regulating branching and tiling of da neurons (Emoto et al., 2004, 2006). Sax-1 and Sax-2 have been found to serve a similar role in *C. elegans* mechanosensory neurons (Gallegos and Bargmann, 2004). In *trc* and *fry* mutants, all classes of da neurons display dendritic overbranching, while class IV da neurons additionally exhibit dendritic crossing of isoneuronal branches (one feature of self-avoidance defects) and dendritic crossing between neighboring class IV neurons (tiling defects) (Emoto et al., 2004). It is not known whether self-avoidance and tiling employ the same dendrite recognition and avoidance mechanism.

One candidate for mediating dendritic interactions is Dscam, a type I membrane protein of the immunoglobulin superfamily (Schmucker et al., 2000). Alternative usage of 12 exon 4, 48 exon 6, and 33 exon 9 variants coding for parts of the extracellular Ig domains, as well as 2 alternative exons for the transmembrane segment, yields a total of 38,016 possible splice variants of Dscam—most of which have been detected in vivo (Neves et al., 2004; Watson et al., 2005; Zhan et al., 2004). Strong homophilic interactions are only observed between the same isoforms of Dscam (Wojtowicz et al., 2004), raising the possibility that isoform-specific interactions contribute to the intricate patterning within the nervous system. Interestingly, different combinations of Dscam isoforms are found in neighboring neurons of the same type (Neves et al., 2004; Zhan et al., 2004). Moreover, *Dscam* mutants display abnormal axonal targeting and axonal branch segregation (Hummel et al., 2003; Wang et al., 2002), and even a modest reduction of Dscam diversity alters mechanosensory neuronal projections (Chen et al., 2006). Loss of *Dscam* function also reduces the dendritic field of olfactory projection neurons, leading to the suggestion that Dscam may have a role in mediating dendritic repulsion (Zhu et al., 2006). It is therefore of particular interest to analyze individual da neurons for *Dscam* loss of function and misexpression phenotypes to assess the role of Dscam in self-avoidance, tiling, and the coexistence of overlapping dendritic fields.

In this study, we examined the cell-autonomous function of Dscam by employing Mosaic Analysis with a Repressible Cell Marker (MARCM). We found that loss of *Dscam* function caused self-avoidance defects in all four da neuron classes, resulting in crossing and bundling of dendrites in clones of individual *Dscam* mutant da neurons. In contrast, self-avoidance in class I–III da neurons did not require *trc* function, and loss of *trc* function caused dendritic crossing, but not bundling, in class IV neurons. All da neurons lacking Dscam also displayed abnormal coverage of the dendritic field, perhaps partly due to the failure in self-avoidance. However, adjacent class IV da neurons lacking *Dscam* function still exhibited tiling. Thus, *Dscam* is required for self-avoidance, but probably not tiling. Self-avoidance and dendritic field coverage in *Dscam* mutant animals were restored to a large extent in class I and IV da neurons expressing any of four arbitrarily chosen full-length Dscam isoforms, but not in those expressing Dscam lacking the intracellular domain. Remarkably, whereas duplicated class I neurons normally showed extensive overlap of their dendrites, overexpression of a single Dscam isoform restricted their sharing of dendritic fields. Moreover, expression of the same Dscam isoform in all da neurons led to dendritic avoidance between the different classes, thus strongly reducing their dendritic field overlap. We conclude that while a single Dscam isoform is sufficient for self-avoidance, Dscam diversity appears to be necessary to ensure coexistence of da neuron dendrites sharing the same territory.

RESULTS

Dscam Function Is Essential for Self-Avoidance and Proper Dendritic Field Coverage of da Neurons

To test whether Dscam function in da neurons is important for dendrite morphogenesis, we first determined whether Dscam is expressed in da neurons by carrying out the following two experiments. First, we used a 4.5 kb Dscam promoter fragment fused to Gal4, which has been shown to reflect the endogenous Dscam expression pattern in the central nervous system (Wang et al., 2004), to drive expression of the reporter mCD8-GFP, and found reporter expression in all four classes of da neurons (see Figure S1A in the Supplemental Data). Next, we confirmed Dscam expression in da neurons with immunofluorescence using an antibody against Dscam revealing a punctate pattern of endogenous Dscam in both axons and dendrites of all da neurons in wild-type (Figure S1B), but not *Dscam* mutant (Figure S1C), larvae.

To specifically remove *Dscam* function in individual da neurons, we used the MARCM technique (Lee et al., 2000) to generate da neuron clones homozygous for either of two mutant alleles known to yield no detectable Dscam protein, $Dscam^{18}$ and $Dscam^{P1}$ (Schmucker et al., 2000; Wang et al., 2002). When mutant for *Dscam*, each class of da neurons displayed dendritic self-avoidance defects in third-instar larvae.

Wild-type MARCM clones of class I da neurons project stereotypical, well-spaced comb-like dendrites to the segmental boundary (Grueber et al., 2002); the dorsal class I ddaD neuron extends its dendrites toward the anterior boundary (not shown), and the dorsal class I ddaE

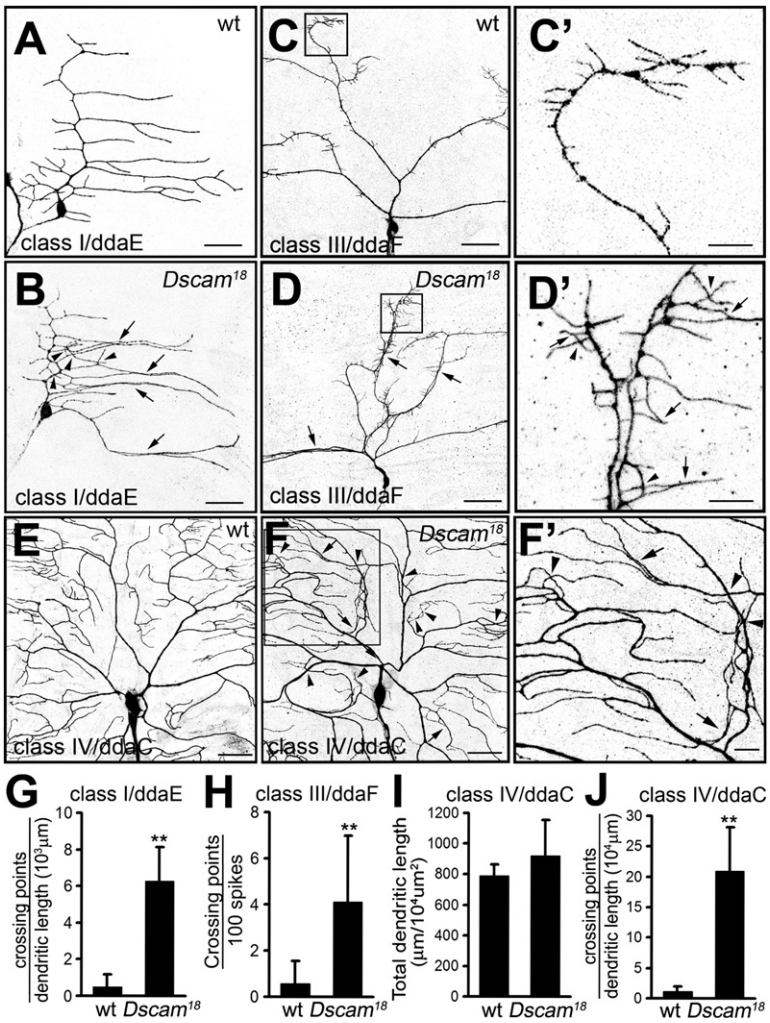

Figure 1. MARCM Analysis of Dendritic Morphogenesis of *Dscam* Mutant da Neurons

(A–F) Representative MARCM clones of class I ddaE (A–B), class III ddaF (C–D), and class IV ddaC (E–F) neurons. Wild-type and *Dscam*^{18} mutant MARCM clones are shown as indicated. (C'), (D'), and (F') are enlarged views of the highlighted areas in (C), (D), and (F). Arrows indicate dendritic bundling and arrowheads indicate crossings of dendritic branches (or crossing of spikes in ddaF). Scale bars, 30 μm in (A)–(F) or 10 μm in (C'), (D'), and (F').

(G–J) Quantitative analysis of the crossing points of class I ddaE dendrites (G, n = 7 for each group), dendritic spikes of ddaF (H, n = 7 for each group), and total dendritic length (I) and the crossing points of dendritic branches (J) of ddaC neurons (n = 6 for each group). All the data are mean ± SD (**p < 0.01, Student's t test).

neuron projects to the posterior boundary (Figure 1A). In contrast, the dendritic branches of individual *Dscam* mutant class I da neurons were often fasciculated (arrows, Figure 1B) or crossed one another (arrowheads, Figures 1B and 1G and Figure S2D). Thus, whereas the dendrites initially projected in the right direction, a failure of self-avoidance resulted in an uneven and abnormal coverage of the dendritic field.

Similar phenotypes were found in mutant clones of class II and class III da neurons. We observed partial bundling of primary and higher order dendritic branches (arrows, Figures 1D and 1D' and Figures S2B, S2C, and S2E). Moreover, whereas dendritic spikes (short, actin-rich dendritic protrusions found only in class III neurons [Andersen et al., 2005]) of control MARCM clones of class III da neurons did not cross (Figures 1C and 1C', and Grueber et al., 2003), the spikes in *Dscam* mutant clones frequently crossed (arrowheads, Figures 1D, 1D', and 1H) or bundled together (arrows, Figure 1D'). This suggests that dendritic spikes as well as dendritic branches require Dscam function for self-avoidance.

The *Dscam* mutant phenotype was further analyzed in class IV da neurons, which display the most complex dendrite morphology. Compared with control MARCM clones that exhibited extensive dendritic field coverage but virtually no crossing between isoneuronal dendrites (Figure 1E), loss of *Dscam* function in class IV da neurons led to frequent crossing (arrowheads) and bundling (arrows) of dendritic branches (Figures 1F and 1F' and Figure S2F). There was a 10-fold increase in dendritic crossings (Figure 1J) but no significant alteration in overall dendritic length (Figure 1I). It thus appears that Dscam is required for self-avoidance of all classes of da neurons.

Dscam Does Not Play a Major Role in Tiling between Dendrites of Neighboring Class IV da Neurons

Given that avoidance of crossing between dendrites of the same or neighboring class IV da neurons requires the NDR kinase Tricornered (Trc), its activator Furry (Fry), and its upstream kinase, the tumor suppressor Hippo (Hpo) (Emoto et al., 2004, 2006), it is of interest to determine

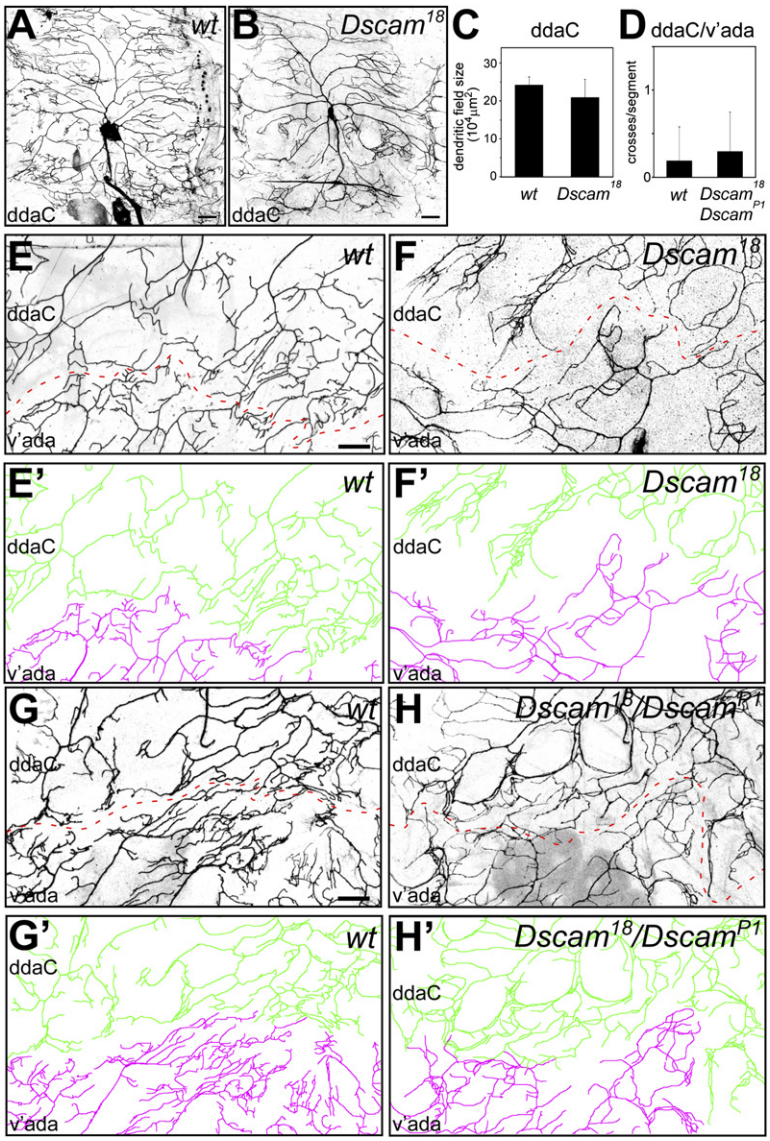

Figure 2. Dscam Does Not Play a Major Role in Interneuronal Recognition and Tiling

(A and B) MARCM clones of wild-type (A) and *Dscam*^{18} mutant (B) class IV ddaC neurons. Note that the dendritic field size is largely unchanged in *Dscam* mutants (B) compared with that of the wild-type (A) and does not show prominent overgrowth.

(C) Quantitative analysis of total dendritic field size of wild-type (n = 4) and *Dscam*^{18} (n = 5) ddaC MARCM clones. Data are mean ± SD. n.s., Student's t test.

(D) Quantitative analysis of interneuronal dendritic crosses between adjacent ddaC and v'ada class IV da neurons in wild-type (n = 16) and *Dscam*^{18}/*Dscam*^{P1} (n = 17) third-instar larvae. Data are mean ± SD. n.s., Student's t test.

(E and F) Dendrites of two adjacent MARCM clones of wild-type (E and E') and *Dscam*^{18} mutant (F and F') ddaC (green, E' and F') and v'ada (magenta, E' and F') neurons form a boundary (indicated by dashed lines) without showing any overlap.

(G and H) The boundary between dendrites of adjacent ddaC and v'ada neurons is shown for wild-type (G and G') and *Dscam*^{18}/*Dscam*^{P1} (H and H') third-instar larvae. ddaC (green, G' and H') and v'ada (magenta, G' and H') neurons form a boundary (indicated by dashed lines) without showing major overlap or crossing of dendrites. Scale bar, 30 μm.

whether Dscam is required for tiling as well as self-avoidance.

Tiling mutants typically display abnormally enlarged dendritic fields, the result of a decrease in dendritic growth inhibition (Emoto et al., 2004). In class IV da neuron clones mutant for *Dscam*, however, despite abnormal field coverage, the dendritic field did not exhibit signs of overgrowth and its size was comparable with that of control MARCM clones (Figures 2A–2C).

Furthermore, we looked for the relatively rare events of two adjacent class IV da neuron MARCM clones homozygous for *Dscam* mutations. We found that neighboring ddaC (dorsal) and v'ada (ventral') mutant neurons displayed fairly normal tiling (n = 3, Figures 2F and 2F'). Although we observed rare dendritic branch crossings (data not shown), overall the tiling of adjacent mutant clones resembled the tiling of neighboring control MARCM class IV da neuron clones (Figures 2E and 2E').

To provide a more thorough quantitative analysis with a larger sample number, we also analyzed tiling in larvae carrying the transheterozygous combination of *Dscam*^{18}/*Dscam*^{P1} alleles, since they can survive to the third instar stage. We used *ppk-Gal4, UAS-mCD8-GFP* to specifically visualize class IV neurons and examined the adjacent dendritic fields of the v'ada and ddaC class IV neurons for interneuronal crossing defects. Similar to the MARCM analysis, virtually no crossing of dendrites from neighboring neurons was observed in wild-type (Figures 2D, 2G, and 2G'). Likewise, in the *Dscam* mutant larvae, despite extensive isoneuronal dendrite crossing and bundling, no significant increase in interneuronal crossing of v'ada and ddaC dendrites was observed (Figures 2D, 2H, and 2H'). The rare crossing or touching of interneuronal dendrites was

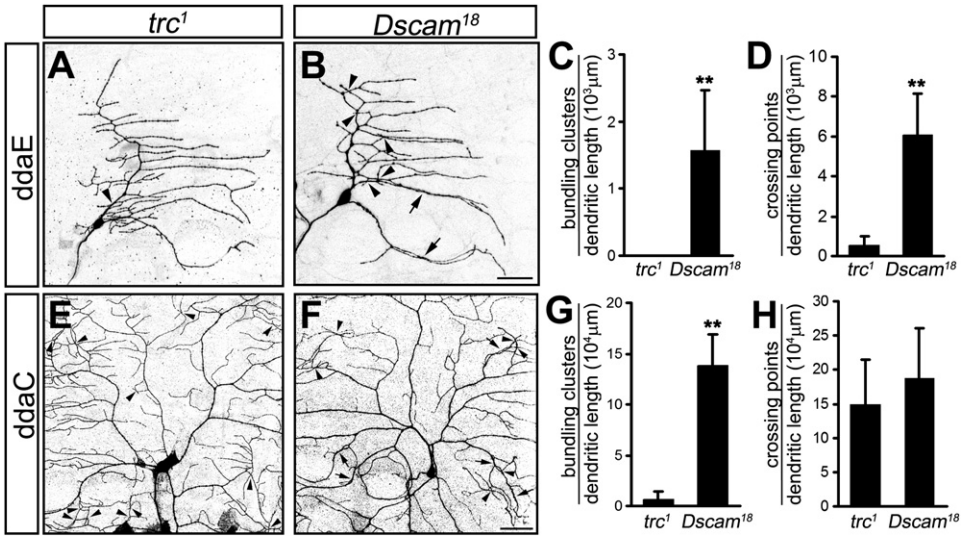

Figure 3. *trc* Function Is Not Required for Self-Avoidance in Class I da Neurons and Prevention of Dendritic Bundling in Class IV da Neurons

(A–D) MARCM clones of class I ddaE neurons mutant for *trc*^{1} (A) and *Dscam*^{18} (B) are shown, and dendritic bundling (C) and crossing (D) were quantified for both genotypes. Dendritic bundling events were defined as physical contact between two or more branches over a distance of more than 5 μm. Scale bar, 30 μm. Data are mean ± SD. **p < 0.01, Student's t test.

(E–H) MARCM clones of class IV ddaC neurons mutant for *trc*^{1} (E) and *Dscam*^{18} (F) are shown, and dendritic bundling (G) and crossing (H) were quantified for both genotypes. While both *trc* and *Dscam* loss of function caused crossing defects, bundling of dendrites was only observed in the *Dscam* mutant. Scale bar, 30 μm. Data are mean ± SD. **p < 0.01, Student's t test.

often associated with bundling and therefore likely represents a secondary effect rather than a real tiling phenotype. These results support the notion that Dscam is required for self-avoidance, but not tiling, of dendrites from adjacent class IV da neurons.

The Hpo/Trc/Fry Pathway Does Not Mediate Self-Avoidance in Class I–III da Neurons or Prevention of Class IV da Neuron Dendritic Bundling

Dscam function in da neurons ensures self-avoidance by preventing dendritic crossing and bundling. To examine whether *trc* also contributes to self-avoidance, we compared the MARCM phenotypes of *Dscam* with *trc* mutants with respect to dendrite crossing and bundling in class I and IV da neurons.

Dscam mutant class I da neurons showed crossing and bundling of dendrites as described above (Figure 3B). As expected of *trc* function in dendritic branching (Emoto et al., 2004), we observed overbranching proximal to the soma in *trc* mutant ddaE neurons (Figure 3A). However, *trc* mutant class I da neurons exhibited no dendritic crosses or bundling (Figures 3A, 3C, and 3D). Moreover, we found no evidence for self-avoidance defects in class I da neurons in *hpo* or *fry* mutants (data not shown). This suggests that the Hpo/Trc/Fry signaling pathway is not required for self-avoidance of class I da neuron dendrites. Similarly, no self-avoidance defects were detected in *trc* or *hpo* mutant class II and III da neurons (data not shown).

Class IV da neurons mutant for *Dscam* or *trc* showed isoneuronal dendritic crossing as previously described (Figures 3E, 3F, and 3H) (Emoto et al., 2004). However, unlike *Dscam* mutants, *trc* mutant class IV da neurons did not exhibit significant dendritic bundling (Figure 3G). We also found no bundling defects in class IV da neurons in *hpo* or *fry* mutant animals (data not shown). Thus, the Hpo/Trc/Fry pathway is not required to prevent dendrite bundling of class IV da neurons or self-avoidance of class I–III da neurons.

Expression of Single Dscam Isoforms Significantly Restored Self-Avoidance and Normal Dendritic Projection

Neurons in wild-type animals typically express multiple isoforms of Dscam (Neves et al., 2004; Zhan et al., 2004). While expression of a single Dscam isoform was sufficient to rescue axonal branch segregation in mushroom body neurons (Wang et al., 2002; Zhan et al., 2004), it proved insufficient to rescue the axonal projections of *Drosophila* mechanosensory neurons (Chen et al., 2006). However, given that self-avoidance involves dendritic interactions within a single neuron, we wondered whether the homophilic interaction of a single isoform of Dscam is sufficient to restore self-avoidance of *Dscam* mutant da neurons. We tested this possibility in several transgenic lines, with each carrying a randomly selected Dscam isoform with or without a C-terminal GFP tag.

First, we generated lines expressing Dscam isoforms carrying the alternative transmembrane exons 17.1 (TM1) and 17.2 (TM2) in class IV da neurons using the *ppk-Gal4* driver. Although the ectopic expression might

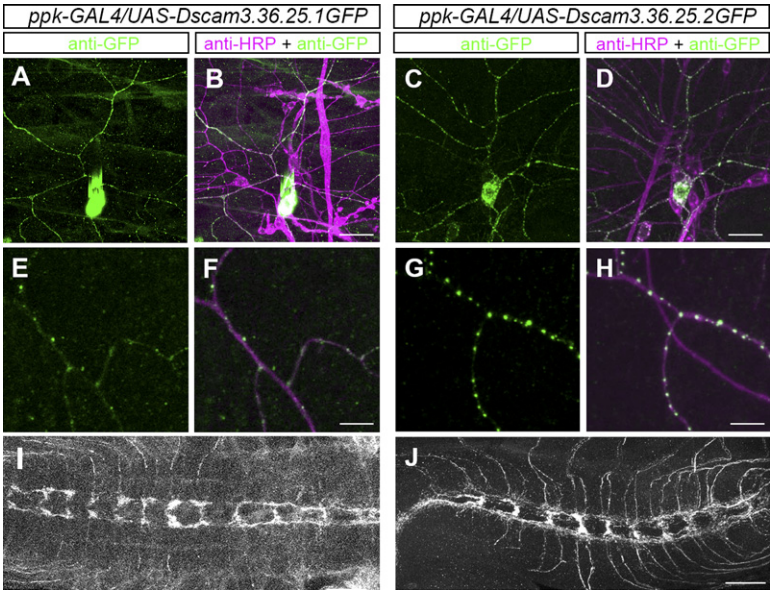

Figure 4. Subcellular Localization of TM1 and TM2 Dscam Isoforms

(A–J) The transgenic GFP-tagged Dscam isoforms TM1 (3.36.25.1) and TM2 (3.36.25.2) were expressed in class IV da neurons using *ppk-Gal4*. The somato-dendritic distribution pattern of GFP-labeled TM1 (A) and TM2 (C) isoforms in ddaC neurons is shown, and it is overlaid with staining using the anti-HRP antibody, a panneuronal membrane marker (Jan and Jan, 1982) (B and D). Scale bar, 30 μm. (E–H) Enlarged view of a ddaC dendritic segment showing a punctate pattern of TM1 (E) and TM2 (G) Dscam isoforms and merged with anti-HRP staining (F and H). Scale bar, 30 μm. TM1 (I) and TM2 (J) isoform expression was also detected in class IV axonal projections in the VNC. Scale bar, 10 μm.

not completely reflect the endogenous localization pattern, previous studies have shown a distinct localization pattern of TM1 and TM2 isoforms in mushroom body neurons (Wang et al., 2004; Zhan et al., 2004). TM1 isoforms localize preferentially to the somato-dendritic compartment, while TM2 isoforms localize to both dendritic and axonal compartments. In class IV da neurons, the TM1 isoform (3.36.25.1GFP) was primarily localized to the soma, but was also present in punctuate structures in dendrites (Figures 4A, 4B, 4E, and 4F). This TM1 isoform was also found at low levels in the class IV axon terminals (Figure 4I). The same TM1 isoform (3.36.25.1) without a GFP tag showed a similar localization pattern in dendrites and axons as revealed by Dscam antibody staining (Figure S3). The TM2 isoform (3.36.25.2) localized to a similar extent to both axons and dendrites of class IV da neurons (Figures 4C, 4D, and 4J), although in dendrites, it was present in larger puncta (Figures 4G and 4H) as compared with the TM1 isoform (Figures 4E and 4F).

Besides the two isoforms with identical extracellular domains, we generated additional lines expressing Dscam isoforms with different extracellular domains and tested their ability to rescue the self-avoidance defects in class I and class IV da neurons as well. Using *Gal4*$^{2\text{-}21}$, *UAS-mCD8-GFP* to visualize class I da neurons, or *ppk-Gal4, UAS-mCD8-GFP* to delineate class IV neurons, we observed dendritic bundling and dendrite crossing phenotypes in *Dscam*^{18}/*Dscam*^{P1} larvae (Figure 5B and Figure 6B), similar to the self-avoidance defects observed in MARCM clones of *Dscam* mutant da neurons. In *Dscam* mutant class I neurons, expression of a single Dscam isoform under the control of *Gal4*$^{2\text{-}21}$ largely restored wild-type morphology of class I ddaE neurons (Figures 5C–5E). The number of isoneuronal dendritic crosses (Figure 5G) and bundling defects (Figure 5H) was significantly reduced upon expression of each of five Dscam transgenes tested in our analysis. Notably, dendritic self-avoidance was restored to a similar extent by Dscam isoforms with three different extracellular domains and TM1 or TM2 transmembrane domains (Figures 5G and 5H). In contrast, Dscam lacking the intracellular domain, Dscam (3.36.25.1ΔC), was not able to rescue dendrite crossing and bundling (Figures 5F, 5G, and 5H), indicating that intracellular signaling via the Dscam C-terminal domain is required for self-avoidance.

Similarly, in class IV da neurons, the expression of a single isoform of Dscam rescued dendritic self-avoidance to a large extent (Figures 6G and 6H); in rescued *Dscam* mutant larvae (Figures 6C–6E), the number of dendritic crosses and bundling defects in ddaC neurons expressing each of the tested Dscam isoforms was comparable with that of wild-type (Figure 6A) and significantly lower than that in *Dscam* mutant larvae (Figure 6B). Furthermore, class IV da neurons expressing a single Dscam isoform displayed an overall dendritic field coverage resembling that of wild-type with little or no dendrite bundling when compared with *Dscam* mutants (Figures 6C–6E). In contrast, expression of Dscam(3.36.25.1ΔC) did not rescue dendritic crosses or bundling (Figures 6F, 6G, and 6H) even though it showed a comparable expression and localization pattern (data not shown). Instead, it led to aberrant targeting, especially of terminal dendrites, with the dendritic tips frequently touching and adhering to neighboring branches (Figure 6F). These results indicate that while a single full-length isoform of Dscam is sufficient for self-avoidance of class IV da neurons, the lack of the Dscam intracellular domain results in a loss of signaling required for repulsion.

Loss of *Dscam* function also affected the axonal projections of class IV da neurons in the ventral nerve cord (VNC), which could be partially restored by expression of a single Dscam isoform (Figure S4).

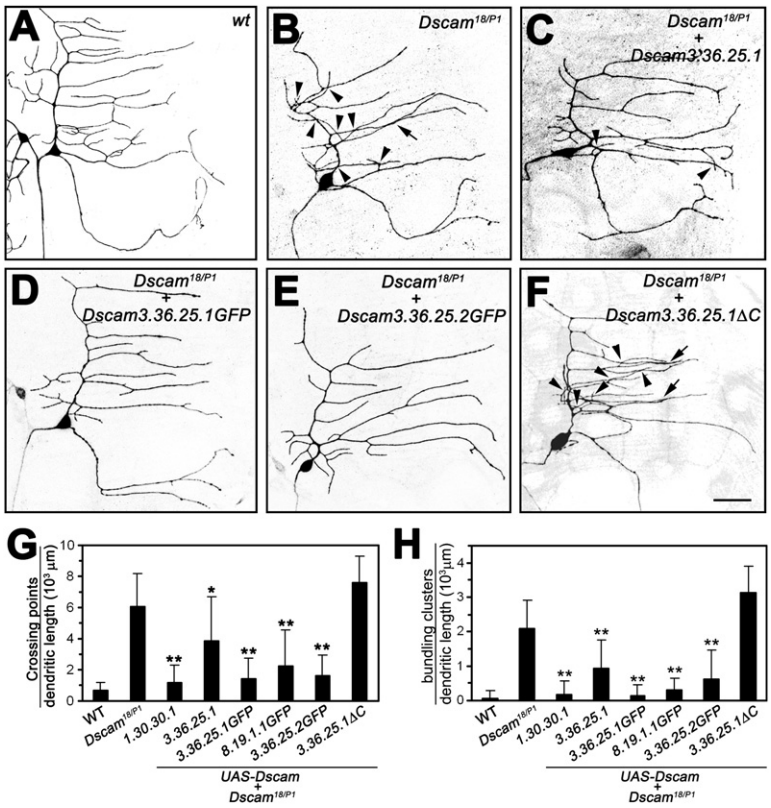

Figure 5. Introduction of Single Dscam Isoforms into the *Dscam* Mutant Background Substantially Rescues Class I Dendrite Crossing and Bundling

(A–F) Class I ddaE neurons visualized by the expression of *UAS-mCD8-GFP* driven by the class-I-specific $Gal4^{2\text{-}21}$ in third-instar larvae. Wild-type (A, n = 12), $Dscam^{18}/Dscam^{P1}$ (B, n = 16), and $Dscam^{18}/Dscam^{P1}$ expressing *UAS-Dscam (3.36.25.1)* (C, n = 9), *UAS-Dscam (3.36.25.1GFP)* (D, n = 16), *UAS-Dscam (3.36.25.2GFP)* (E, n = 10), or *UAS-Dscam (3.36.25.1ΔC)* (F, n = 13) under the control of $Gal4^{2\text{-}21}$ are shown. Arrowheads indicate dendritic branch crossing and arrows indicate bundling events.

(G and H) Quantitative analysis of dendritic crosses (G) and bundling (H) of the indicated genotypes [sample number as indicated above; for *UAS-Dscam (1.30.30.1)*, n = 8, and for *UAS-Dscam (8.19.1.1GFP)*, n = 10)]. Self-avoidance defects of *Dscam* mutant ddaE neurons were significantly reduced by all overexpressed Dscam isoforms when compared with those of *Dscam* mutant ddaE neurons alone. Data are mean ± SD; *p < 0.05, **p < 0.01, one-way ANOVA.

Avoidance of Dendrites of Duplicated Class I da Neurons Overexpressing the Same Dscam Isoform

Having found that a single isoform of Dscam could largely restore dendritic self-avoidance, we tested whether expression of the same Dscam isoform in neurons that normally do not avoid one another could induce avoidance of their dendrites. It was previously found that duplicated class I da neurons in *hamlet* mutants show no avoidance toward each other, but rather exhibit similar dendritic projection patterns with extensive overlap (Grueber et al., 2003). We obtained similar results by shifting a temperature-sensitive *Notch* mutant (N^{ts}) to the restrictive temperature for 1–2 hr during early embryonic development, resulting in duplication of about one in ten ventral class I da neuron (vpda) neurons. As in *hamlet* mutants, duplicated vpda neurons in N^{ts} larvae extended dendritic arbors of normal shape and size that overlapped extensively (Figures 7A, 7A', 7B, and 7B'). Nonduplicated vpda neurons in the same animals had identical morphology to wild-type vpda neurons in control animals (Figure S5). Thus, the transient inactivation of *Notch* did not affect vpda dendrite development, but provided an opportunity to examine dendritic interactions between the duplicated class I neurons. In contrast to the extensive overlap between duplicated control neuron dendrites, expression of a single Dscam isoform (3.36.25.1GFP) in the duplicated vpda neurons led to separation of their dendritic fields, with dendrites of the neighboring neurons avoiding each other (Figures 7C, 7C', 7D, and 7D').

We quantified the length and number of secondary branches of duplicated vpda neurons growing either toward ("in") or away ("out") from each other (Figures 7E and 7F) and the number of branch crosses between the two neurons (Figure 7G). Duplicated control vpda neurons readily grew toward each other and their dendrites crossed extensively. In contrast, duplicated vpda neurons expressing the same Dscam isoform preferentially branched away from each other and exhibited greatly reduced dendrite crossing, while the average length of secondary branches remained unaltered (Figures 7F and 7G). In the same animals, nonduplicated vpda neurons expressing Dscam did not exhibit a preference in the direction of branching (Figure S5). It thus appears that the presence of the same isoform of Dscam in the duplicated neurons is sufficient for their dendrites to avoid one another and force a switch in branching directionality.

Expression of the Same Dscam Isoform in Different Classes of da Neurons Prevents the Overlap of Their Dendritic Fields

Having found that expression of a common Dscam isoform prevented duplicated class I da neurons from sharing the same dendritic field, we wondered whether such avoidance behavior could be conferred to neurons of different classes that normally overlap in their dendritic field coverage. If expression of the same Dscam isoform in different classes of da neurons prevented them from innervating the same region of the body wall, this undesirable

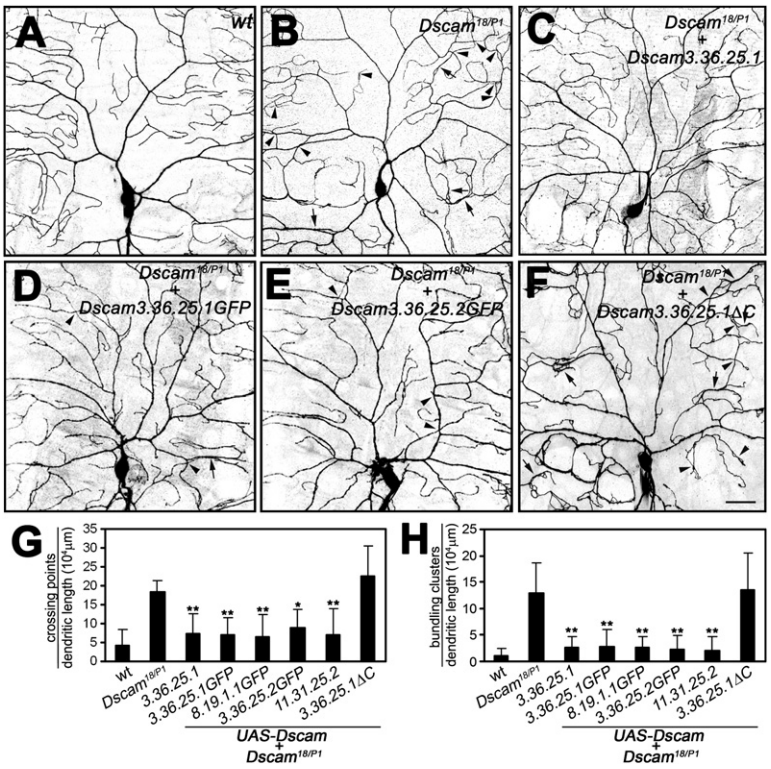

Figure 6. Introduction of Single Dscam Isoforms into the *Dscam* Mutant Background Substantially Rescues Class IV Dendrite Crossing and Bundling

(A–F) Class IV ddaC neurons visualized via the expression of *UAS-mCD8-GFP* driven by class-IV-specific *ppk-Gal4*. Wild-type (A, n = 6), $Dscam^{18}/Dscam^{P1}$ (B, n = 6), and $Dscam^{18}/Dscam^{P1}$ expressing *UAS-Dscam (3.36.25.1)* (C, n = 8), *UAS-Dscam (3.36.25.1GFP)* (D, n = 9), *UAS-Dscam (3.36.25.2GFP)* (E, n = 6), or *UAS-Dscam (3.36.25.1ΔC)* (F, n = 8) are shown. Arrowheads indicate dendritic branch crossings and arrows indicate bundling events. Scale bars, 30 µm. Note that expression of a single Dscam isoform in class IV neurons significantly rescued the *Dscam* loss-of-function phenotype with regard to dendritic crossing and bundling in ddaC neurons.

(G and H) Quantitative analysis of crossing points (G) and bundling events (H) of class IV ddaC neurons of the indicated genotypes (sample number as indicated above, and for *UAS-Dscam (11.31.25.2)*, n = 8). Self-avoidance defects of *Dscam* mutant ddaC neurons were significantly reduced by all overexpressed Dscam isoforms when compared with those of *Dscam* mutant ddaC neurons alone. Data are mean ± SD; $^{**}p < 0.01$, one-way ANOVA.

outcome would provide one rationale for the existence of a very large number of Dscam splice variants; namely, it would ensure self-avoidance without significant risk of neighboring neurons inadvertently expressing a common Dscam isoform.

To address this question, we used the pan-da $Gal4^{21\text{-}7}$ driver to specifically express each of four different Dscam isoforms in all da neurons. During development, the class I vpda neuron is the first ventral da neuron to project dendrites dorsally, followed by the dendritic growth of neighboring class II, III, and IV neurons, whose dendrites substantially overlap those of the vpda neurons (Figures 8A and 8A'). Remarkably, pan-da neuronal overexpression of a single Dscam isoform with either the TM1 or TM2 transmembrane domain greatly reduced the overlap and crossing of dendrites from different classes of da neurons (Figures 8B, 8B', 8C, and 8C'). The dendritic field established early on by the vpda neuron remained nearly devoid of other neuronal dendrites, acting as a barrier for ventral neurons projecting to the posterior segment boundary. In addition, some of the neighboring neurons showed enlarged dendritic terminals (Figure 8B', arrows) indicative of stalled dendritic growth. In da neurons expressing a common Dscam isoform, the number of heteroneuronal dendritic crosses with the vpda neuron was consistently reduced. Comparable results were obtained for each of the four Dscam isoforms tested (Figure 8D).

To look more closely into the behavior of da neuronal dendrites growing toward the vpda class I dendrites, we carried out time-lapse imaging of da neurons expressing GFP-tagged Dscam (8.19.1.1) driven by the pan-da $Gal4^{80G2}$ driver in embryos, starting at stage 17, when the class I vpda neuron has established its dendritic field and neighboring dendrites begin to extend (Figure 8E, 0 min). In these animals, the dendrites of neighboring neurons growing toward the vpda field retracted once they came into close proximity (Figure 8E, 45 and 105 min). Moreover, even after reinitiation of growth, they failed to extend into the vpda dendritic field (Figure 8E, 180 min), an avoidance behavior never observed in control embryos. These results show that expression of a common Dscam isoform induces avoidance and severely compromises the ability of different classes of da neurons to cover the same territory.

Coexistence of Overlapping Dendritic Fields Is Impaired in Animals Expressing Only a Single Dscam Isoform

To further confirm that a single common Dscam isoform prevents coexistence of overlapping da neuron dendritic fields, we reduced the multiplicity of Dscam isoforms by expressing only a single isoform in all da neurons in *Dscam* mutant animals. For this purpose, we used $Dscam^{18}/Dscam^{P1}$ mutant animals carrying a 4.5 kb *Dscam* promoter fragment fused to Dscam (3.36.25.1), and *ppk-Gal, UAS-CD8-GFP* to mark class IV da neurons. The 4.5 kb Dscam promoter fragment has previously been shown to reflect the endogenous Dscam expression pattern (Wang et al., 2004) and to be specific for pan-da neuronal expression in the peripheral nervous system (PNS)

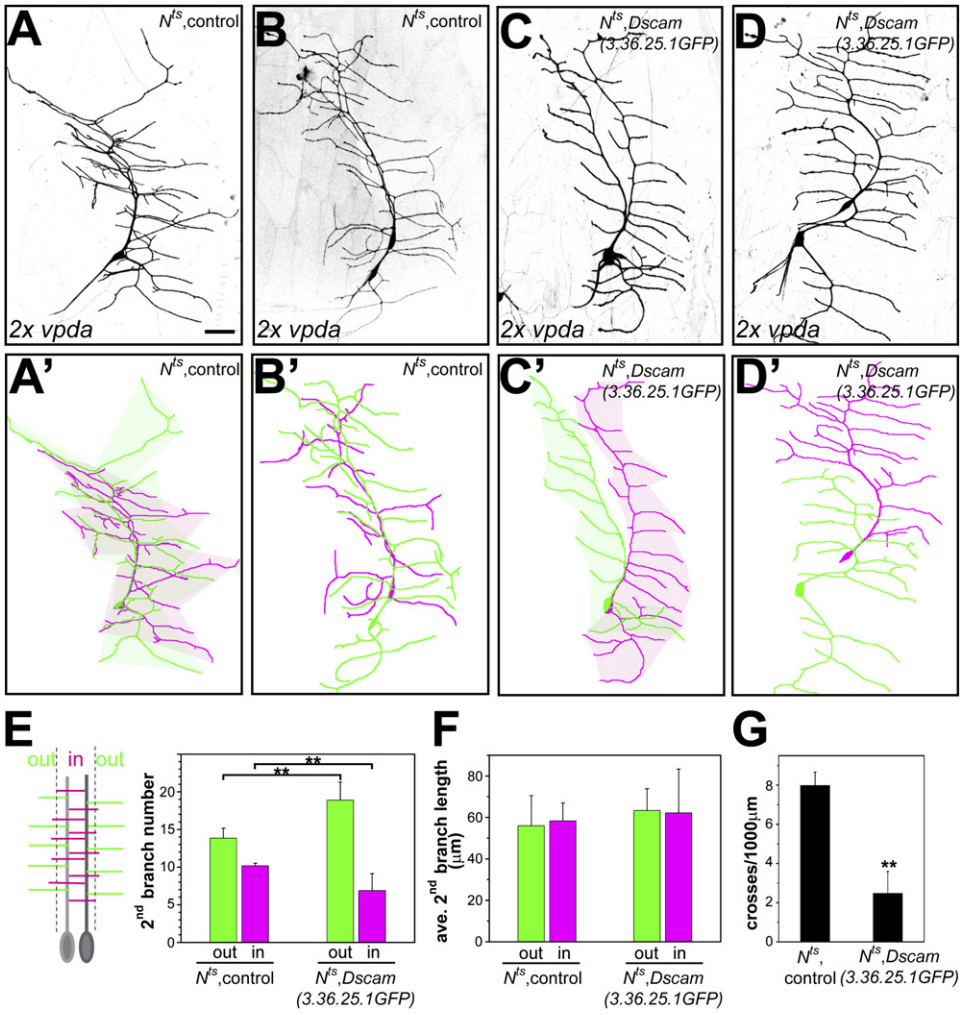

Figure 7. Ectopic Expression of a Single Dscam Isoform Induces Recognition and Repulsion of Duplicated vpda Neurons

(A–D) Class I vpda neurons were duplicated using the temperature-sensitive N^{ts} allele with a 1–2 hr shift to the restrictive temperature during embryonic development and visualized in third-instar larvae with *Gal4*$^{2\text{-}21}$ driven *UAS-mCD8-GFP*. Two examples are shown each for N^{ts}, control (A and B) and N^{ts}, *UAS-Dscam (3.36.25.1GFP)* (C and D); their corresponding color-coded tracings are shown in (A')–(D'). Dendritic fields of duplicated vpda neurons expressing the same Dscam isoform show avoidance and highly reduced dendritic field overlap, as indicated by the shaded colored areas representing each individual dendritic field (A' and C'). Scale bar, 30 μm.

(E–G) Quantitative analysis of Dscam-induced repulsion. Secondary branches (2nd) of duplicated vpda neurons were classified according to those branching away from (''out'') or towards (''in'') each other. The number (E) and length (F) of secondary in and out branches and the number of interneuronal dendritic crosses (G) were determined for each vpda pair of the indicated genotype (n = 8 for each group). Data are mean ± SD; **p < 0.01, Student's t test.

(see Figure S1). Immunostaining with anti-CD8/anti-GFP and anti-HRP antibodies allowed us to visualize class IV da neurons and all sensory neurons (Jan and Jan, 1982), respectively, in the periphery.

In wild-type (Figure 9A) and *Dscam* mutant animals (data not shown), the ventral class IV vdaB neuron and ventral' v'ada neuron together covered the entire ventral field. The dendritic fields of these class IV da neurons completely overlapped with the class I vpda dendritic field (Figures 9A' and 9A''). Remarkably, expression of a single isoform under the control of the *Dscam* promoter in the *Dscam* mutant background resulted in avoidance and partial exclusion of class IV dendrites (Figure 9B) from the vpda dendritic field (Figures 9B' and 9B''). Although expression of a single common Dscam isoform also reduced self-avoidance defects in all da neurons, it concomitantly caused inter-class avoidance. Quantitative analysis of *Dscam* mutant animals expressing a single Dscam isoform revealed that dendritic crosses (Figure 9C) and dendritic field overlap (Figure 9D) between class IV (vdaB, v'ada) and class I (vpda) da neurons was significantly reduced compared with that of wild-type, reflecting an inability of class I and class IV da neurons to cover the same territory.

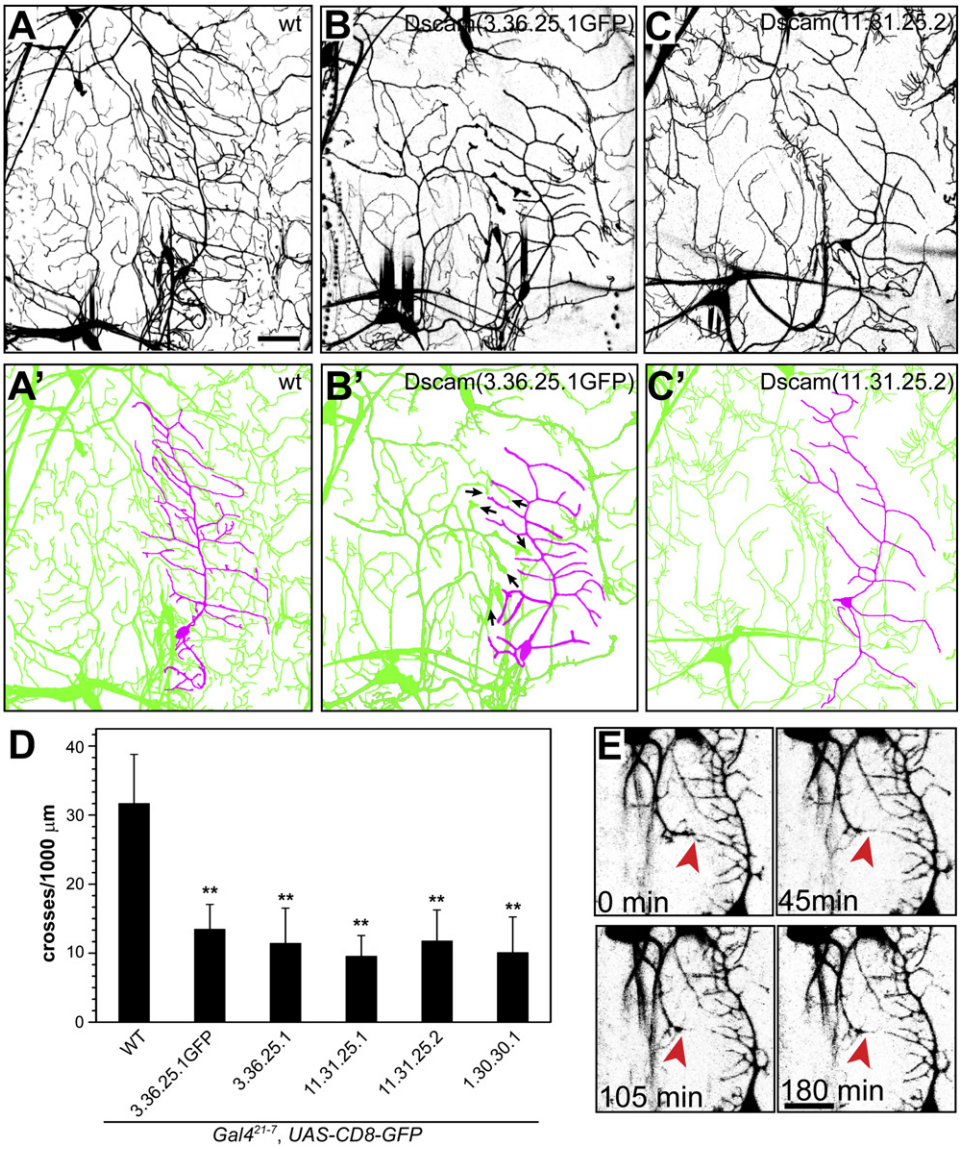

Figure 8. Ectopic Expression of Single Dscam Isoforms Induces Heteroneuronal Recognition and Repulsion

(A–C) The pan-da neuronal driver *Gal4*$^{21\text{-}7}$ driving *UAS-mCD8-GFP* allowed visualization of da neurons at the third instar larval stage. The wild-type (A), *UAS-Dscam (3.36.25.1GFP)* (B), and *UAS-Dscam (11.31.25.2)* (C) overexpressing ventral and ventral' da neuron clusters and their corresponding tracings (A', B', and C') are shown. The vpda class I neuron is traced in magenta and the ventral and ventral' class II, II, and IV neurons are shown in green. Arrows in (B') mark enlarged dendritic terminals indicative of stalled dendritic growth. Scale bar, 30 μm.

(D) Quantitative analysis of Dscam-induced repulsion between ventral da neurons. Heteroneuronal dendritic crossing points between vpda dendrites and other ventral da neurons were counted and normalized to the total dendritic length of the vpda neuron for each genotype as indicated. n = 13 in each group. Data are mean ± SD; **p < 0.01, one-way ANOVA.

(E) Time-lapse images of stage 17 embryos overexpressing GFP-tagged Dscam (8.19.1.1) in all da neurons under the control of *Gal4*^{80G2}. Growing dendrites from the v'ada class IV neuron are repelled by vpda class I neuron dendrites and fail to penetrate the vpda dendritic field (indicated by red arrowheads). Scale bar, 20 μm.

Similarly, we observed avoidance between dendrites of the dorsal da neuron cluster using the same *Dscam* promoter-driven Dscam isoform in the *Dscam* mutant background (Figure S6). Here, ddaC class IV neuron dendrites avoided other da neuron dendrites, resulting in dendritic growth parallel to or around other da neuron dendrites. In severe cases, the failure of coexistence compromised the ability of ddaC neurons to cover the entire dorsal field (Figure S6C). Our results therefore show that in animals expressing only a single Dscam isoform, da neuron dendrites recognize and avoid each other. Thus, a lack of Dscam diversity severely impaired

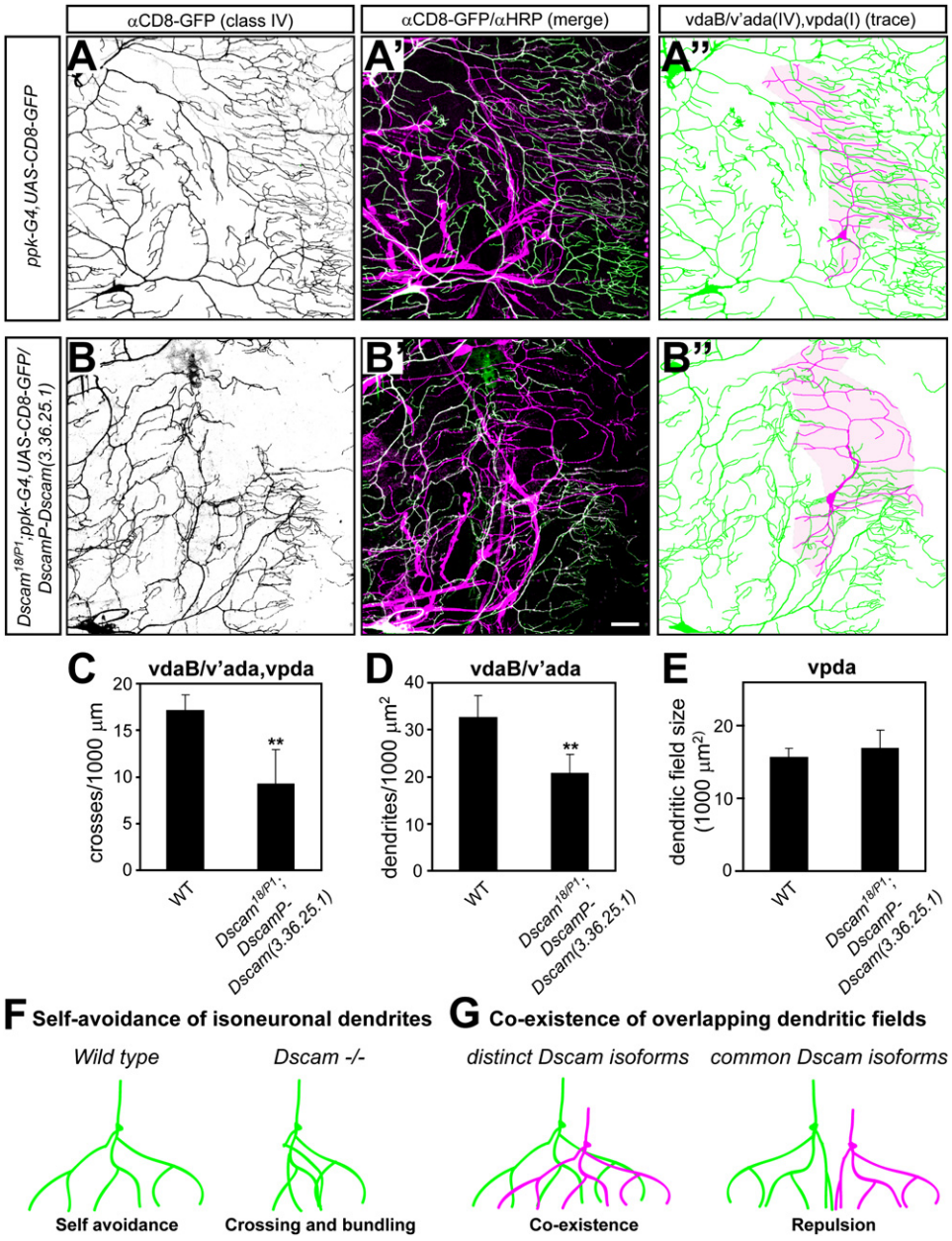

Figure 9. Coexistence of Overlapping da Neuron Dendritic Fields Is Impaired in Larvae Expressing Only a Single Dscam Isoform

(A–E) Comparison of class IV (vdaB and v'ada) da neuron field coverage and overlap with that of the class I (vpda) neuron in wild-type (A) and *Dscam*^{18}/*Dscam*^{P1}*; DscamP-Dscam (3.36.25.1)* (B) third-instar larvae carrying *ppk-Gal, UAS-CD8-GFP*. Larvae of both genotypes were immunostained with anti-CD8/anti-GFP and anti-HRP antibodies to visualize class IV da neurons (A and B) and all sensory neurons (merge with anti-CD8/GFP shown in [A'] and [B']), respectively. Corresponding tracings of the vpda class I neuron (magenta) and class IV (vdaB, v'ada) neurons (green) are shown for each genotype (A'' and B''). The vpda dendritic field is indicated by the shaded area (magenta). Scale bar, 30 µm. Dendritic crosses (C, n = 6), dendritic field overlap between class IV (vdaB, v'ada) and class I (vpda) da neurons (D, n = 6), and class I vpda dendritic field size (E) were quantified for each genotype as indicated. Data are mean ± SD; **p < 0.01, Student's t test.

(F and G) Dscam plays a pivotal role in dendritic self-avoidance and coexistence of overlapping dendritic fields. Self-avoidance of da neuron dendrites requires at least a single isoform of Dscam to ensure nonredundant and even target field coverage. The lack of Dscam, which causes a loss of self-recognition and subsequent repulsion, leads to extensive crossing and bundling of dendrites (F). Dscam diversity is required to allow different types of neurons to innervate overlapping fields, as observed for the different types of da neurons. Expression of a common Dscam isoform leads to dendrite recognition and avoidance, resulting in nonoverlapping dendritic fields (G).

coexistence of da neuron dendritic fields in the same territory.

DISCUSSION

We have identified Dscam as a key molecule for mediating dendritic self-avoidance in all four classes of da neurons. Loss of *Dscam* function resulted in excessive crossing and bundling of dendrites, accompanied by an uneven coverage of the dendritic field. These defects can be substantially corrected by the expression of each of four arbitrarily chosen Dscam isoforms. Our findings reveal that Dscam is critical for neurons to evenly extend their dendrites to cover the appropriate dendritic field, and to avoid the potential ambiguity arising from having different dendritic branches respond to the same input.

Given the necessity for different classes of da neurons to express at least one isoform of Dscam to ensure self-avoidance, it is important to explore the possible consequences of having multiple da neurons in the same region express the same Dscam isoform. Different classes of da neurons presumably respond to different sensory inputs, and hence their coverage of overlapping regions of the body wall will allow the animal to detect different types of sensory stimuli at the same physical locations. We found that the expression of a common Dscam isoform made it almost impossible for different classes of da neurons to occupy the same territory, which is likely associated with deprivation of all but one type of sensory input at any one location. These considerations provide a plausible explanation for the existence of a vast number of Dscam splice variants (Neves et al., 2004; Zhan et al., 2004). For Dscam to mediate self-recognition manifested as dendritic self-avoidance in da neurons, it may be crucial to limit the expression of each of the Dscam isoforms to one or a small subset of neurons in any region of the nervous system. This allows neighboring neurons to interact in ways distinct from the interactions that occur between isoneuronal processes of an individual neuron. Indeed, microarray analyses of individual *Drosophila* photoreceptor cells and mushroom body neurons have found distinct Dscam isoforms expressed in neighboring cells (Neves et al., 2004; Zhan et al., 2004). This supports the idea that an intricate splicing mechanism ensures that individual neurons can distinguish between self and nonself (Celotto and Graveley, 2001; Graveley, 2005; Neves et al., 2004). Given that divergent Dscam isoform expression is required for coexistence of da neurons in the same territory, it is likely that other mechanisms are involved in recognition of neighboring class IV da neurons for the purpose of tiling.

Intriguingly, even duplicated class I neurons most likely express distinct Dscam isoforms, since they occupy the same territory, but repel each other when expressing a common Dscam isoform. While the specific isoforms expressed by individual da neurons are currently unknown, the general principle of enabling dendrites of a single neuron to avoid one another without imposing recognition and avoidance of neighboring neurons underscores the importance of Dscam diversity. Since Dscam has been shown to primarily interact in an isoform-specific manner (Wojtowicz et al., 2004), Dscam-based self-recognition and self-avoidance depends on expression of the same isoforms. This is illustrated by the repulsive function of Dscam in vivo, where it induces branch retraction and avoidance of dendrites expressing identical isoforms (see Figures 8B, 8C, and 8E). The self-avoidance phenomenon seems to be conserved in axonal development as well: in mushroom body neurons *Dscam* ensures the proper segregation and targeting of the two axonal processes to different lobes (Wang et al., 2002).

Our study reveals significant differences between self-avoidance, which encompasses isoneuronal crossing and bundling of dendrites, and tiling. *Dscam* is essential for dendritic self-avoidance (dendritic crossing and bundling) of all classes of da neurons, but not for tiling of class IV da neurons. Thus, different recognition mechanisms are used for self-avoidance and tiling. The phenomenon of tiling, in which the dendrites of different neurons of the same class avoid one another, relies on components of the Hpo/Trc/Fry pathway (Emoto et al., 2004, 2006). Whereas this signaling pathway also contributes to the avoidance of isoneuronal dendritic crossing of class IV da neurons, it is not required to prevent bundling of class IV da neuron dendrites, nor is it important for self-avoidance of the other three classes of da neurons. It is an interesting open question as to what intracellular machineries are employed to prevent the dendrites of each da neuron in class I–III from crossing one another. The involvement of the Hpo/Trc/Fry pathway in preventing crossing, but not bundling, of dendrites from the same class IV da neuron further suggests the possibility of multiple mechanisms for self-avoidance. While fasciculation of multiple processes, e.g., those in axon guidance, is a widely used mechanism to ensure accurate projection to common target areas (Van Vactor, 1998), bundling of isoneuronal dendrites defeats the purpose of dendritic field coverage and nonredundant signal processing. Given the ample opportunities for neighboring dendritic branches of the same neuron to bundle, there is likely a specialized mechanism that repels branching dendrites from each other as they respond to cues for their extension.

EXPERIMENTAL PROCEDURES

Fly Stocks

Dscam^{18}, *Dscam*^{P1}, (Hummel et al., 2003; Schmucker et al., 2000; Wang et al., 2002), and *trc*^{1}, *hpo*^{mgh4} (Emoto et al., 2006; Geng et al., 2000) mutant alleles have been described previously. The Dscam transgenic lines carrying the isoforms (3.36.25.1), (3.36.25.1GFP), (3.36.25.2GFP), (8.19.1.1GFP), (11.31.25.1), (11.31.25.2), (1.30.30.1), and (3.36.25.1ΔC) used in this study have been described (Wang et al., 2004; Zhu et al., 2006). Transgenic lines with the 4.5 kb Dscam promoter fragment fused to Gal4 (*DscamP-Gal4*) or Dscam (3.36.25.1) [*DscamP-Dscam (3.36.25.1)*] have been described in Wang et al. (2004).For visualization of class IV da neurons, a fusion of the *pickpocket* (*ppk*) enhancer (Grueber et al., 2003) to Gal4 was used to drive expression of mCD8-GFP. *Gal4*$^{2\text{-}21}$, *UAS-mCD8-GFP*

was used to visualize class I da neurons (Parrish et al., 2006). The panda lines *Gal4*$^{21\text{-}7}$ (Song et al., 2007) and *Gal4*^{80G2} (Gao et al., 1999) were used to visualize all da neurons and to overexpress the different individual Dscam isoforms. The *N*^{ts} allele has been described in Shellenbarger and Mohler (1975).

MARCM Analysis

MARCM analyses were essentially performed as described previously (Grueber et al., 2002). Briefly, *FRT*^{G13} *Dscam*^{18}, *UAS-mCD8-GFP/CyO* or *FRT*^{G13} *Dscam*^{P1}, *UAS-mCD8-GFP/CyO* flies were mated with *w, elav-Gal4, hs-Flp; FRT*^{G13}, *tub-Gal80/CyO* to generate mosaic clones. Analogously, *FRT*^{42D} *hpo*^{mgh4} and *FRT*^{80B} *trc*^{1} flies were mated with the corresponding *w, elav-Gal4, hs-Flp; FRT*^{42D}, *tub-Gal80/CyO* or *w, elav-Gal4, hs-Flp; FRT*^{80B}, *tub-Gal80/CyO*, respectively. Embryos were collected for 2 hr at 25°C and allowed to develop for 3 hr, then heat shocked for 1 hr at 38°C. Heat-shocked embryos were kept at 25°C and da neuron MARCM clones were analyzed in third-instar larvae by immunohistochemistry.

Immunohistochemistry

Antibodies used in this study were as follows: rat-anti-mCD8 antibody (1:100, Invitrogen, San Diego), mouse-anti-Dscam targeted against exon 18 (1:100), and Cy5-mouse-anti-HRP (1:200, Jackson IR Labs, West Grove). Immunohistochemistry of *Drosophila* larvae was preformed essentially as described in Grueber et al. (2002). Briefly, third-instar larvae were dissected and fixed in 4% formaldehyde/PBS and stained with the desired primary antibodies. Appropriate secondary antibodies coupled to Cy2, Rhodamine red, or Cy5 were purchased from Jackson IR. Filets were mounted in Slowfade gold (Invitrogen, San Diego) and analyzed by confocal microscopy on a Leica TCS SP2 microscope. Z-stacks of confocal sections were taken and maximized projections were used for quantitative analysis. For clarity and best reproduction of dendritic processes, images were inverted and contrast-enhanced using Photoshop (Abobe Systems Inc., San Jose). Dendritic length and terminal branch numbers were quantified using the ImageJ (NIH, Bethesda) plug-in NeuronJ (Meijering et al., 2004).

Genetic Duplication of Class I Neurons

N^{ts} females were crossed to *Gal4*$^{2\text{-}21}$, *UAS-mCD8-GFP* with or without *UAS-Dscam-GFP(3.36.25.1)*. Embryos were collected for 1 hr at 20°C and allowed to develop for 3–4 hr, and were then transferred to the restrictive temperature of 29°C for 1–2 hr. Embryos were allowed to develop at 20°C and male third-instar larvae (*N*^{ts}*/Y; Gal4*$^{2\text{-}21}$, *UAS-mCD8-GFP/+* or *N*^{ts}*/Y; UAS-Dscam-GFP(3.36.25.1)/+; Gal4*$^{2\text{-}21}$, *UAS-mCD8-GFP/+*) were analyzed for duplication of class I neurons by confocal microscopy.

Supplemental Data

The Supplemental Data for this article can be found online at http://www.neuron.org/cgi/content/full/54/3/403/DC1/.

ACKNOWLEDGMENTS

We thank Wes Grueber, Larry Zipursky, and Dietmar Schmucker for communicating results prior to publication. We thank members of the Jan lab for discussion; Jill Wildonger and Yi Zheng for comments on the manuscript; Hsiu-Hsiang Lee and Yang Xiang for *Gal4*$^{21\text{-}7}$, *UAS-CD8-GFP*; Jay Parrish for the *N*^{ts} duplication procedure; and Liqun Luo and Haitao Zhu for Dscam reagents. This work was supported by NIH grant RO1 NS40929. L.Y.J. and Y.-N.J. are Investigators of the Howard Hughes Medical Institute.

Received: October 20, 2006
Revised: February 15, 2007
Accepted: March 16, 2007
Published: May 2, 2007

REFERENCES

Amthor, F.R., and Oyster, C.W. (1995). Spatial organization of retinal information about the direction of image motion. Proc. Natl. Acad. Sci. USA *92*, 4002–4005.

Andersen, R., Li, Y., Resseguie, M., and Brenman, J.E. (2005). Calcium/calmodulin-dependent protein kinase II alters structural plasticity and cytoskeletal dynamics in Drosophila. J. Neurosci. *25*, 8878–8888.

Celotto, A.M., and Graveley, B.R. (2001). Alternative splicing of the Drosophila Dscam pre-mRNA is both temporally and spatially regulated. Genetics *159*, 599–608.

Chen, B.E., Kondo, M., Garnier, A., Watson, F.L., Puettmann-Holgado, R., Lamar, D.R., and Schmucker, D. (2006). The molecular diversity of Dscam is functionally required for neuronal wiring specificity in Drosophila. Cell *125*, 607–620.

Emoto, K., He, Y., Ye, B., Grueber, W.B., Adler, P.N., Jan, L.Y., and Jan, Y.N. (2004). Control of dendritic branching and tiling by the Tricornered-kinase/Furry signaling pathway in Drosophila sensory neurons. Cell *119*, 245–256.

Emoto, K., Parrish, J.Z., Jan, L.Y., and Jan, Y.N. (2006). The tumour suppressor Hippo acts with the NDR kinases in dendritic tiling and maintenance. Nature *443*, 210–213.

Gallegos, M.E., and Bargmann, C.I. (2004). Mechanosensory neurite termination and tiling depend on SAX-2 and the SAX-1 kinase. Neuron *44*, 239–249.

Gao, F.B., Brenman, J.E., Jan, L.Y., and Jan, Y.N. (1999). Genes regulating dendritic outgrowth, branching, and routing in Drosophila. Genes. Dev. *13*, 2549–2561.

Gao, F.B., Kohwi, M., Brenman, J.E., Jan, L.Y., and Jan, Y.N. (2000). Control of dendritic field formation in Drosophila: the roles of flamingo and competition between homologous neurons. Neuron *28*, 91–101.

Geng, W., He, B., Wang, M., and Adler, P.N. (2000). The tricornered gene, which is required for the integrity of epidermal cell extensions, encodes the Drosophila nuclear DBF2-related kinase. Genetics *156*, 1817–1828.

Graveley, B.R. (2005). Mutually exclusive splicing of the insect Dscam pre-mRNA directed by competing intronic RNA secondary structures. Cell *123*, 65–73.

Grueber, W.B., Jan, L.Y., and Jan, Y.N. (2002). Tiling of the Drosophila epidermis by multidendritic sensory neurons. Development *129*, 2867–2878.

Grueber, W.B., Ye, B., Moore, A.W., Jan, L.Y., and Jan, Y.N. (2003). Dendrites of distinct classes of Drosophila sensory neurons show different capacities for homotypic repulsion. Curr. Biol. *13*, 618–626.

Hummel, T., Vasconcelos, M.L., Clemens, J.C., Fishilevich, Y., Vosshall, L.B., and Zipursky, S.L. (2003). Axonal targeting of olfactory receptor neurons in Drosophila is controlled by Dscam. Neuron *37*, 221–231.

Jan, L.Y., and Jan, Y.N. (1982). Antibodies to horseradish peroxidase as specific neuronal markers in Drosophila and in grasshopper embryos. Proc. Natl. Acad. Sci. USA *79*, 2700–2704.

Jan, Y.N., and Jan, L.Y. (2003). The control of dendrite development. Neuron *40*, 229–242.

Lee, T., Winter, C., Marticke, S.S., Lee, A., and Luo, L. (2000). Essential roles of Drosophila RhoA in the regulation of neuroblast proliferation and dendritic but not axonal morphogenesis. Neuron *25*, 307–316.

Meijering, E., Jacob, M., Sarria, J.C., Steiner, P., Hirling, H., and Unser, M. (2004). Design and validation of a tool for neurite tracing and analysis in fluorescence microscopy images. Cytometry A *58*, 167–176.

Neves, G., Zucker, J., Daly, M., and Chess, A. (2004). Stochastic yet biased expression of multiple Dscam splice variants by individual cells. Nat. Genet. *36*, 240–246.

Parrish, J.Z., Kim, M.D., Jan, L.Y., and Jan, Y.N. (2006). Genome-wide analyses identify transcription factors required for proper morphogenesis of Drosophila sensory neuron dendrites. Genes. Dev. *20*, 820–835. Published online March 17, 2006. 10.1101/gad.1391006.

Perry, V.H., and Linden, R. (1982). Evidence for dendritic competition in the developing retina. Nature *297*, 683–685.

Rockhill, R.L., Euler, T., and Masland, R.H. (2000). Spatial order within but not between types of retinal neurons. Proc. Natl. Acad. Sci. USA *97*, 2303–2307.

Schmucker, D., Clemens, J.C., Shu, H., Worby, C.A., Xiao, J., Muda, M., Dixon, J.E., and Zipursky, S.L. (2000). Drosophila Dscam is an axon guidance receptor exhibiting extraordinary molecular diversity. Cell *101*, 671–684.

Shellenbarger, D.L., and Mohler, J.D. (1975). Temperature-sensitive mutations of the notch locus in Drosophila melanogaster. Genetics *81*, 143–162.

Song, W., Onishi, M., Jan, L.Y., and Jan, Y.N. (2007). Peripheral multidendritic sensory neurons are necessary for rhythmic locomotion behavior in Drosophila larvae. Proc. Natl. Acad. Sci. USA *104*, 5199–5204.

Stuart, G., Spruston, N., and Häusser, M. (1999). Dendrites (New York: Oxford University Press).

Sugimura, K., Yamamoto, M., Niwa, R., Satoh, D., Goto, S., Taniguchi, M., Hayashi, S., and Uemura, T. (2003). Distinct developmental modes and lesion-induced reactions of dendrites of two classes of Drosophila sensory neurons. J. Neurosci. *23*, 3752–3760.

Van Vactor, D. (1998). Adhesion and signaling in axonal fasciculation. Curr. Opin. Neurobiol. *8*, 80–86.

Wang, J., Zugates, C.T., Liang, I.H., Lee, C.H., and Lee, T. (2002). Drosophila Dscam is required for divergent segregation of sister branches and suppresses ectopic bifurcation of axons. Neuron *33*, 559–571.

Wang, J., Ma, X., Yang, J.S., Zheng, X., Zugates, C.T., Lee, C.H., and Lee, T. (2004). Transmembrane/juxtamembrane domain-dependent Dscam distribution and function during mushroom body neuronal morphogenesis. Neuron *43*, 663–672.

Wassle, H., Peichl, L., and Boycott, B.B. (1981). Dendritic territories of cat retinal ganglion cells. Nature *292*, 344–345.

Watson, F.L., Puttmann-Holgado, R., Thomas, F., Lamar, D.L., Hughes, M., Kondo, M., Rebel, V.I., and Schmucker, D. (2005). Extensive diversity of Ig-superfamily proteins in the immune system of insects. Science *309*, 1874–1878.

Wojtowicz, W.M., Flanagan, J.J., Millard, S.S., Zipursky, S.L., and Clemens, J.C. (2004). Alternative splicing of Drosophila Dscam generates axon guidance receptors that exhibit isoform-specific homophilic binding. Cell *118*, 619–633.

Zhan, X.L., Clemens, J.C., Neves, G., Hattori, D., Flanagan, J.J., Hummel, T., Vasconcelos, M.L., Chess, A., and Zipursky, S.L. (2004). Analysis of Dscam diversity in regulating axon guidance in Drosophila mushroom bodies. Neuron *43*, 673–686.

Zhu, H., Hummel, T., Clemens, J.C., Berdnik, D., Zipursky, S.L., and Luo, L. (2006). Dendritic patterning by Dscam and synaptic partner matching in the Drosophila antennal lobe. Nat. Neurosci. *9*, 349–355.